Eur J Plant Pathol (2015) 143:25–42
DOI 10.1007/s10658-015-0662-3

A new root-knot nematode *Meloidogyne spartelensis* n. sp. (Nematoda: Meloidogynidae) in Northern Morocco

Nadine Ali · Johannes Tavoillot · Thierry Mateille · Elodie Chapuis · Guillaume Besnard · Ahmed El Bakkali · Carolina Cantalapiedra-Navarrete · Gracia Liébanas · Pablo Castillo · Juan E. Palomares-Rius

Accepted: 15 April 2015 / Published online: 26 April 2015

Abstract Low density of an unknown root-knot nematode was found on wild olive soils at Cape Spartel near Tanger city in northern Morocco. Morphometry, esterase and malate dehydrogenase electrophoretic phenotypes, as well as ribosomal DNA (rDNA) and mitochondrial DNA (mtDNA) sequences demonstrated that this nematode species differs clearly from other previously described root-knot nematodes. The species is herein described, illustrated and named as *Meloidogyne spartelensis* n. sp. This new root-knot nematode can be morphologically distinguished from other *Meloidogyne* spp. by: (i) roundish perineal pattern, dorsal arch low, with fine, sinuous cuticle striae, lateral field faintly visible; (ii) female excretory pore posterior to stylet knobs, EP/ST ratio 1.4-2.0; (iii) second-stage juveniles with hemizonid located 1 to 2 annuli anterior to excretory pore and long, sub-digitate tail; and (iv) males with lateral field composed of four incisures, with areolated outer bands. Phylogenetic trees based on 18S, ITS1-5.8S-ITS2, D2-D3 of 28S rDNA, and partial *coxII*-16S rRNA and *coxI* gene of mtDNA showed that *M. spartelensis* n. sp. belongs to an undescribed root-knot nematode lineage that is clearly separated from other species with resemblance in morphology, such as *M. dunensis*, *M. kralli*, and *M. sewelli*.

Keywords 18S · Bayesian inference · Cytochrome oxidase subunit II · ITS · Maximum likelihood · mtDNA · New species · Plant-parasitic nematodes · rDNA

N. Ali
Plant Protection Department, Faculty of Agriculture, Tishreen University, PO Box 230, Latakia, Syrian Arab Republic

N. Ali · J. Tavoillot · T. Mateille · E. Chapuis
IRD, UMR CBGP (INRA/IRD/CIRAD/Montpellier SupAgro), 755 avenue du Campus Agropolis, CS30016 34988 Montferrier-sur-Lez Cedex, France

E. Chapuis
IRD, UMR IPME (IRD/Université Montpellier 2/CIRAD), 911 avenue Agropolis, BP 64501 34394 Montpellier Cedex 5, France

G. Besnard
CNRS, UMR EDB (UPS, CNRS, ENFA), Université Toulouse III Paul Sabatier, Bâtiment 4R1, 118 Route de Narbonne, 31062 Toulouse cedex 9, France

A. El Bakkali
INRA, UMR APCRPG, BP 578, Meknès, Morocco

C. Cantalapiedra-Navarrete · P. Castillo · J. E. Palomares-Rius (✉)
Instituto de Agricultura Sostenible (IAS), Consejo Superior de Investigaciones Científicas (CSIC), Apdo. 4084, Campus de Excelencia Internacional Agroalimentario, ceiA3, 14080 Córdoba, Spain
e-mail: palomaresje@ias.csic.es

G. Liébanas
Departamento de Biología Animal, Vegetal y Ecología, Universidad de Jaén, Campus 'Las Lagunillas' s/n, Edificio B3, 23071 Jaén, Spain

Introduction

Root-knot nematodes (RKN) of the genus *Meloidogyne* are among nature's most successful plant parasites, being distributed worldwide and encompassing more than 95 nominal species (Moens et al. 2010). These nematodes infect thousands of different herbaceous and woody monocotyledonous and dicotyledonous plants and cause severe losses to numerous agricultural crops and forest plants worldwide (Moens et al. 2010). Root-knot nematodes (*Meloidogyne* spp.) and root-lesion nematodes (*Pratylenchus* spp.) are the most damaging plant-parasitic nematodes of cultivated olive (*Olea europaea* L. subsp. *europaea* var. *europaea*), especially in nurseries (Castillo et al. 2010; Ali et al. 2014). *Meloidogyne* species known to damage olive trees are well adapted to temperate and subtropical areas and include *Meloidogyne arenaria* (Neal 1889) Chitwood 1949; *Meloidogyne baetica* Castillo et al. 2003a, *Meloidogyne hapla* Chitwood 1949, *Meloidogyne incognita* (Kofoid & White 1919) Chitwood 1949, *M. javanica* (Treub 1885) Chitwood 1949 and *Meloidogyne lusitanica* Abrantes and Santos 1991. In orchards, olive trees infected by *Meloidogyne* spp. show yellowing in the highest branches and defoliation (Castillo et al. 2010). These species occur on wild and cultivated olives in southern Spain, and also in nurseries (except for *M. baetica*) (Castillo et al. 2003b). However, plant-parasitic nematodes infecting wild olive have been scarcely studied in the Mediterranean Basin, except for the recent description of the root-lesion nematode *Pratylenchus oleae* Palomares-Rius et al. 2014 in Spain and Tunisia, and the reniform nematode *Rotylenchulus macrosoma* in Spain (Castillo et al. 2003a). Yet, wild olive populations have persisted in western and eastern parts of the Mediterranean Basin since the Late Tertiary (Besnard et al. 2013), and in particular in southern Spain and Morocco where Last Glacial Maximum refugia have been described for many organisms (Médail and Diadema 2009). Natural dispersal of native phytoparasitic nematodes could be limited (due to physical barriers and low migration ability) and communities of such regions are thus expected to be unique with high level of endemism.

Species determination of *Meloidogyne* is complex, difficult and time-consuming even for experts. The application of molecular methods to studies of RKN population structure and systematics have revealed that some long-assumed single species are in fact cryptic species that are morphologically indistinguishable but may be phylogenetically distant to one another (Gamel et al. 2014). Sequences of nuclear ribosomal (rDNA) and mitochondrial DNA (mtDNA) have been used for molecular characterisation and reconstruction of phylogenetic relationships within the genus *Meloidogyne* during the last decade (Powers and Harris 1993; Ziljstra et al. 2000; Adam et al. 2007; Adams et al. 2009; Castillo et al. 2009). The analysis of isozyme electrophoretic patterns, in particular esterase (Est) and malate dehydrogenase (Mdh), as well as several molecular approaches have proved to be a valuable tool for precise identification of *Meloidogyne* species (Blok and Powers 2009). Consequently, current availability of molecular techniques integrated with classical morphological approaches may help to provide tools for differentiating *Meloidogyne* species and can significantly improve and facilitate the routine identification of these nematodes.

Nematode surveys in wild olive soils in northern Morocco revealed very low population levels of a RKN. This RKN appeared morphologically close-related to *M. kralli* Jepson 1983, *M. dunensis* Palomares-Rius et al. 2007 and *M. sewelli* Mulvey and Anderson 1980, which prompted a comparative study among related species. Some reliable diagnostic approaches commonly used to identify and compare certain RKN species such as analyses of isozyme phenotypes and phylogenetic analyses of ribosomal and mitochondrial DNA sequences were included in the study.

This work describes a new *Meloidogyne* species associated with wild olive in northern Morocco as well as its phylogenetic relationship with other RKNs based on Bayesian inference (BI) and maximum likelihood (ML) analyses of sequences from the 18S, ITS1-5·8S-ITS2, D2-D3 of 28S rDNA, and the partial *coxII*-16S of rRNA and *coxI* gene of mtDNA. The undescribed root-knot nematode is herein described as *Meloidogyne spartelensis* n. sp., the species epithet referring to Cap Spartel where it was detected.

Material and methods

Soil sampling, nematode extraction, and *Meloidogyne* spp. detection and rearing

A nematode survey was conducted in March 2012 in wild olive (*Olea europaea* subsp. *europaea* var. *sylvestris* (Mill.) Lehr) soils in northern Morocco

(Cape Spartel; 35.790583°N; 5.924983°W; altitude 16 m), near Tanger city. Soil sub-samples were collected with a shovel from the upper 20 cm of bare soil under each olive tree canopy and mixed to form one 500 dm^3 reference sample. Nematodes were extracted from 250 cm^3 of fresh soil using the elutriation procedure (Seinhorst 1962), and *Meloidogyne* juveniles and males were observed under a stereomicroscope (Leica M165C, ×60 magnification). Tomato (cv. Roma) and olive (cv. Picholine du Languedoc) plantlets were transplanted in the remaining native soil and reared under controlled greenhouse conditions in order to test the infection rate and plant host range of this RKN. No nematode survived on olive cv. Picholine du Languedoc. But several juveniles and males were extracted from the tomato roots placed in a mist chamber (Seinhorst 1950). The *Meloidogyne* population was again reared on tomato in a sandy-peat substrate (2/3-1/3).

Nematode morphological identification

For diagnosis and identification, females were collected from tomato galled roots, while males, eggs and second-stage juveniles (J2) of nematodes were extracted from the rhizosphere by centrifugal-flotation (Coolen 1979) and from feeder roots by blending in a 0.5 % NaOCl solution for 4 min (Hussey and Barker 1973). Specimens for light microscopy (LM) were killed with gentle heat, fixed in a 4 % solution of formaldehyde+ propionic acid and processed to glycerin by Seinhorst's rapid method (Seinhorst 1966). Specimens were examined using a Zeiss III compound microscope with Nomarski differential interference contrast at powers up to 1,000× magnification. Randomly selected specimens of each life-stage were measured. Measurements and drawings were made at the *camera lucida* on glycerine infiltrated specimens. All measurements were expressed in micrometers (μm). All other abbreviations used are as defined in Siddiqi (2000).

Fixed specimens were dehydrated in a gradient ethanol series, critical-point dried, sputter-coated with gold and observed by scanning electron microscopy (SEM) according to Abolafia et al. (2002).

Perineal patterns of mature females were prepared according to standard procedures (Hartman and Sasser 1985). Briefly, root tissues were teased apart with forceps and half spear to remove adult females. The lip and neck regions of the nematode were excised, and the posterior end was cleared in a solution of 45 % lactic acid to remove remaining body tissues. Then, the perineal pattern was trimmed and transferred to a drop of glycerin. At least 50 perineal patterns were examined for species identification.

Isozyme phenotype analysis

To obtain sufficient individuals of *M. spartelensis* n. sp. for electrophoretic analyses, the nematode population under study and a reference *M. javanica* population from olive trees sampled at Córdoba, Spain (Nico et al. 2002), were increased on tomato (cv. Roma) in a glasshouse at 25±3 °C. For that, a single egg mass of *M. spartelensis* n. sp. was placed beneath the roots of individual tomato seedling in 12 cm pots filled with sterile loamy soil. Sixty days after inoculation, tomato plants were uprooted, their roots gently washed free of soil and the root tissues teased apart using forceps and transfer needles to remove adult females.

Five young egg laying females of *Meloidogyne spartelensis* n. sp. and of *M. javanica* (reference population) were macerated in microtubes containing 5 μl of 20 % (*wt/vol*) sucrose, 1 % (*vol/vol*) Triton X-100 and 0·01 % (*wt/vol*) bromophenol blue. Electrophoresis was carried out in 7×8 cm separating (pH 8·4) and stacking (pH 6·8) homogeneous gels, 7 and 4 % polyacrylamide, respectively, 0·75-mm thick, with Tris-glycine buffer in a Mini Protean II electrophoresis unit (BioRad). Gels were stained with the substrate α-naphthyl acetate for Est and with Fast Blue RR (Sigma-Aldrich) for Mdh. Band patterns and relative migration of the bands (Rm) were compared to *M. javanica* (Esbenshade and Triantaphyllou 1985).

Nematode molecular identification

For molecular analyses, one female nematode was temporary mounted in a drop of 1 M NaCl containing glass beads and after taking measurements and photomicrographs of diagnostic characters the slides were dismantled and DNA extracted. Nematode DNA was extracted from single females and PCR assays were conducted as described by Castillo et al. (2003b). The D2-D3 expansion segments of 28S rDNA was amplified using the D2A (5′-ACAAGTACCGTGAGGGAAAGTTG-3′) and D3B (5′-TCGGAAGGAACCAGCTACTA-3′) primers (De Ley et al. 1999). The ITS region was amplified using forward primers 18S (5′-TTGATTAC

GTCCCTGCCCTTT-3′) and 26S (5′-TTTCACTCGC CGTTACTAAGGGAATC-3′) (Vrain et al. 1992). The 18S region was amplified with MelF (5′-TACGGACT GAGATAATGGT-3′) and MelR (5′-GGTTCAAGCC ACTGCGA-3′) as described in Tigano et al. (2005). The region of the mitochondrial genome between the cytochrome oxidase subunit II (*coxII*) and 16S rRNA mitochondrial DNA (mtDNA) genes was amplified using primers C2F3 (5′-GGTCAATGTTCAGAAATT TGTGG-3′) and 1108 (5′-TACCTTTGACCAATCA CGCT-3′) (Powers and Harris 1993). A 450-pb portion of the cytochrome oxidase subunit I gene (*coxI*) of mtDNA was amplified using primers COX1F1 (5′-TTGRTTTTTTGGTCATCCTGARG-3′) and COX1R1 (5′-WSYMACWACATAATAAGTATCAT G-3′). COX1F1 and COX1R1 were designed using PRIMER3 software (http://frodo.wi.mit.edu/primer3/input.htm) from nematode mtDNA sequences (Lazarova et al. 2006).

PCR products were purified after amplification using ExoSAP-IT (Affmetrix, USB products), quantified using a Nanodrop spectrophotometer (Nanodrop Technologies, Wilmington, DE, USA) and used for direct sequencing in both directions using the primers referred above. The resulting products were purified and run on a DNA multicapillary sequencer (Model 3130XL genetic analyser; Applied Biosystems, Foster City, CA, USA), using the BigDye Terminator Sequencing Kit v.3.1 (Applied Biosystems, Foster City, CA, USA), at the Stab Vida sequencing facilities (Caparica, Portugal). *CoxI* PCR products were purified and sequenced in both directions using the primers referred above by Eurofins MWG Company (Germany). The resulting products were corrected and aligned using Geneious R7 v. 7.1.2 (www.geneious.com) and BioEdit (Hall 1999) softwares. The newly obtained sequences were submitted to the GenBank database under accession numbers indicated on the phylogenetic trees.

Phylogenetic analyses

D2-D3 expansion segments of 28S rDNA, ITS rDNA, partial 18S and *coxII*-16S rRNA sequences of different *Meloidogyne* species from GenBank were used for phylogenetic reconstruction. Outgroup taxa for each dataset were chosen according to previous published data (Castillo et al. 2009). The newly obtained and published sequences for each gene were aligned using MAFFT (Katoh et al. 2002) with default parameters. Sequence alignments were manually edited using BioEdit (Hall 1999). Phylogenetic analyses of the sequence data sets were performed based on maximum likelihood (ML) using PAUP * 4b10 (Swofford 2003) and Bayesian inference (BI) using MrBayes 3.1.2 (Ronquist and Huelsenbeck 2003). The best fitted model of DNA evolution was obtained using jModelTest v. 2.1.1 (Darriba et al. 2012) with the Akaike Information Criterion (AIC). The Akaike-supported model, the base frequency, the proportion of invariable sites, and the gamma distribution shape parameters and substitution rates in the AIC were then used in phylogenetic analyses. BI analysis under a general time reversible of invariable sites and a gamma-shaped distribution (GTR+I+G) model for D2-D3 expansion segment of 28S rDNA, (GTR+G) model for ITS1, (GTR+I+G) model for partial 18S and (GTR+I+G) model for *coxII*-16S rRNA, were run with four chains for 2×10^6, 2×10^6, 3×10^6 and 1×10^6 generations, respectively. The Markov chains were sampled at intervals of 100 generations. Two runs were performed for each analysis. After discarding burn-in samples and evaluating convergence, the remaining samples were retained for further analyses. The topologies were used to generate a 50 % majority rule consensus tree. Posterior probabilities (PP) are given on appropriate clades. Trees were visualised using TreeView (Page 1996). In ML analysis the estimation of the support for each node was obtained by bootstrap analysis with 100 fast-step replicates.

Results

Meloidogyne spartelensis[1] n. sp. (Figs. 1, 2 and 3, Table 1)

Holotype (female in glycerin) Body length L=712 μm; maximum body width=409 μm; a=1.5; stylet length=14.5 μm; dorsal pharyngeal gland opening (DGO)=3.5 μm; excretory pore from anterior end=21.5 μm; excretory pore distance from anterior end/length of stylet (EP/ST)=1.5; vulva slit length=22 μm; distance from vulva to anus=26.5 μm.

[1] The species epithet is derived from Cape Spartel, the locality from which the new species was collected.

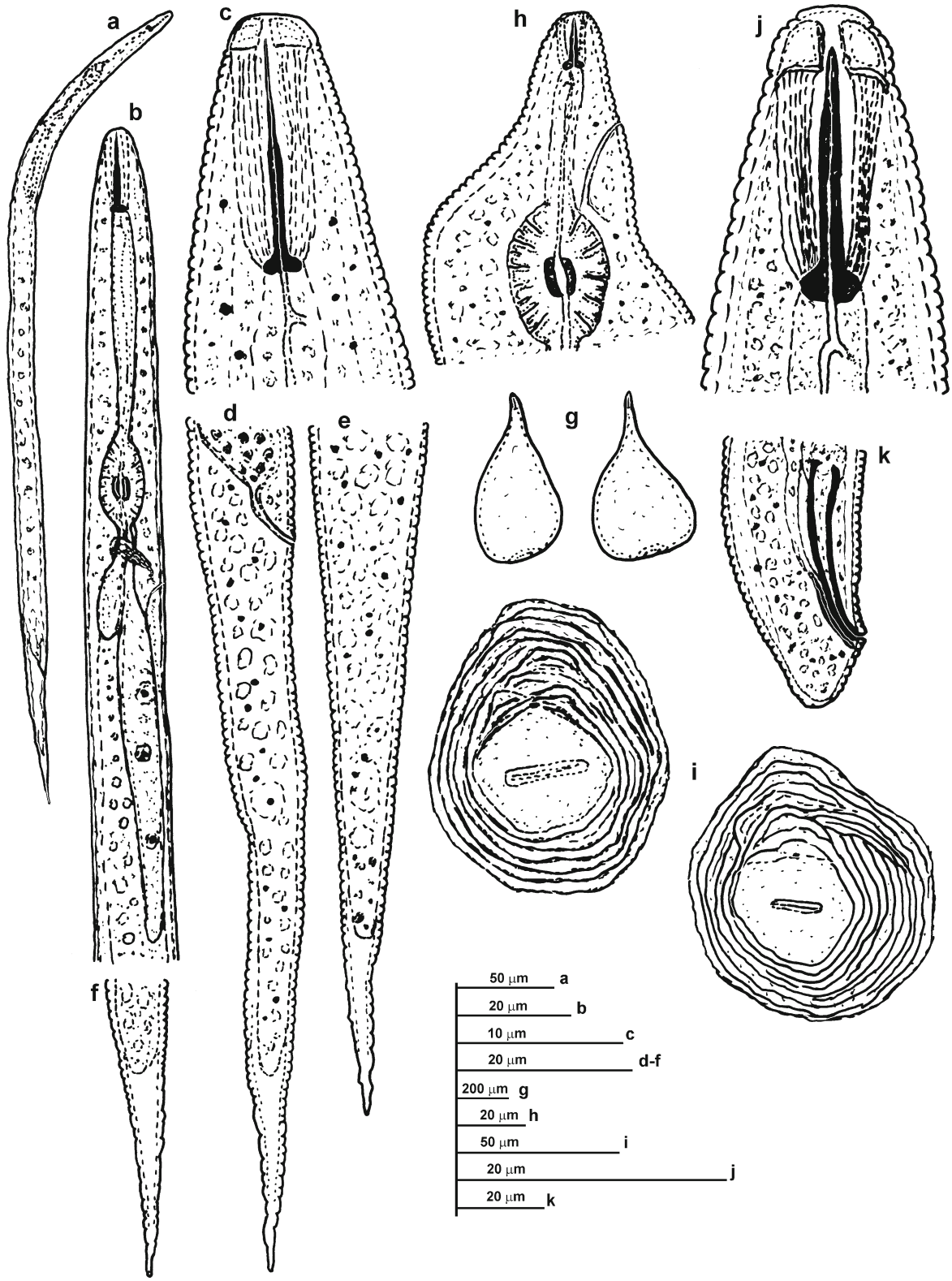

Fig. 1 Line drawings of *Meloidogyne spartelensis* n. sp. from Morocco. Second-stage juvenile (**a-f**). **a** Whole body. **b** Pharyngeal region. **c** Lip region. **d-f** Tail regions. Female (**g-i**). **g** Whole females. **h** Lip region. **i** Perineal patterns. Male (**j-k**). **j** Lip region. **k** Tail region

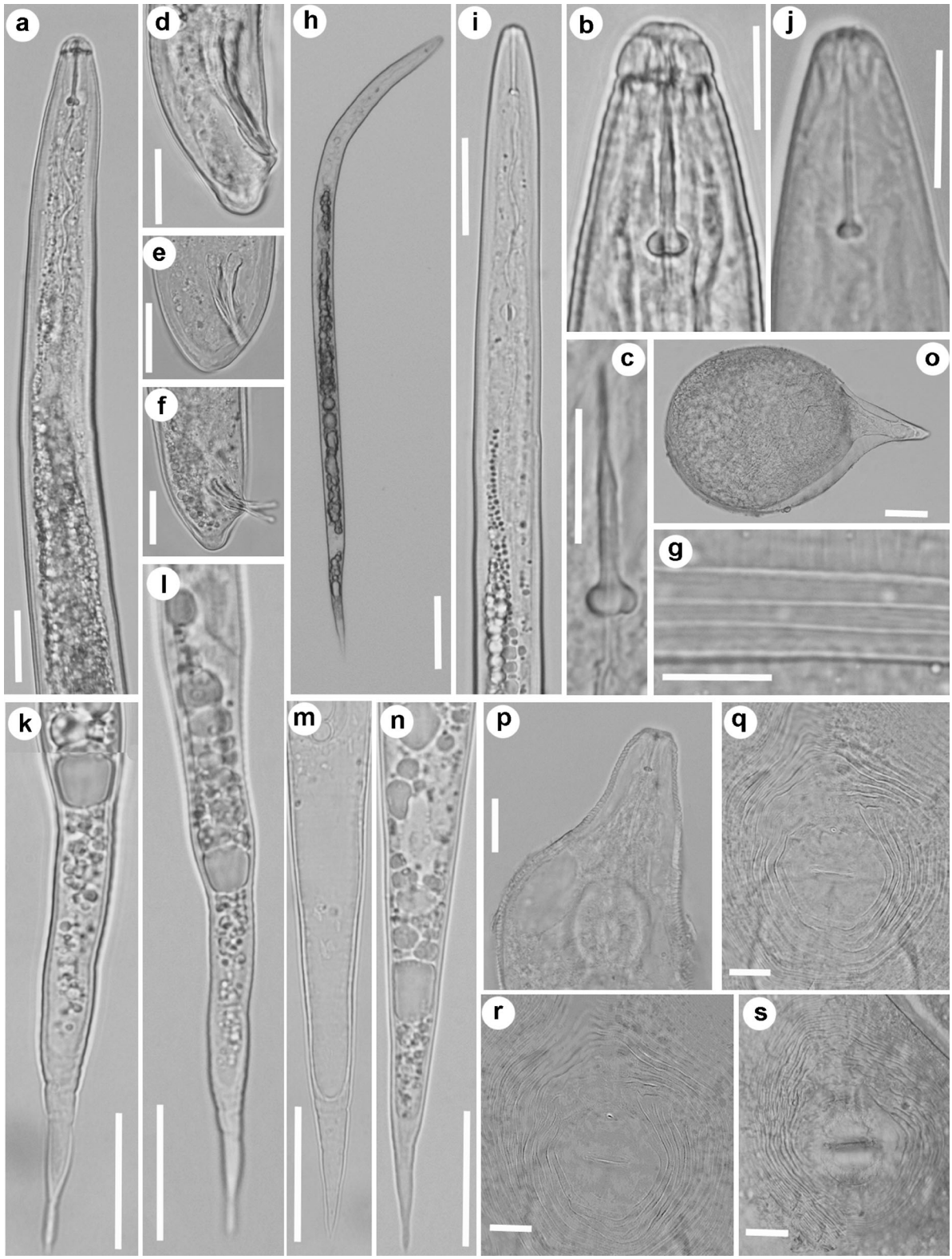
a
d
h
i
b
j
e
c
o
f
g
l
k
m
n
p
q
r
s

Fig. 2 Light micrographs of *Meloidogyne spartelensis* n. sp. from Morocco. Male (**a-g**). **a** Pharyngeal region. **b** Lip region. **c** Detail of stylet. **d-f** Tail region showing spicules and gubernaculum. **g** Lateral field at mid-body. Second-stage juvenile (**h-n**). **h** Whole Second-stage juvenile. **i** Pharyngeal region. **j** Lip region. **k-n** Tail regions. Mature female (**o-s**). **o** Whole female. **p** Female neck region. **q-s** perineal pattern. (Scale bars: **a**, **d-f**, **k-n**, **p-s**=20 μm; **b**, **c**, **g**, **j**=10 μm; **h**=50 μm; **o**=100 μm)

Female paratypes (*n*=16) L=621±89 (489–772) μm; maximum body width=386±45 (267–455) μm; a=1.6 ±0.1 (1.4–1.8); stylet length 15.1±0.3 (14.5–15.5) μm; excretory pore from anterior end 23.1±2.2 (21.0–30.0) μm; EP/ST ratio (excretory pore to head end/stylet length)=1.5±0.1 (1.4–2.0); vulva slit=22.0±1.6 (18.0–25.0) μm; vulva-anus distance=21.3±2.2 (16.5–35.0) μm.

Female Body usually completely embedded in galled tissue in tomato, pearly white body, varying in shape from ovoid to saccate and with a variable neck diam. and length (Figs. 1g to 2o). Lip region continuous with body contour. Head cap variable in shape, with labial disk and post labial annulus not elevated. In SEM view, the labial disc appears round-squared, slightly raised on the medial and lateral sectors, which are all fused together (Fig. 3a and b). Labial framework weakly sclerotized. Amphidial apertures elongated, located between labial disc and lateral lips. Stylet fairly long, with an almost straight, rarely curved, cone, cylindrical shaft and knobs oval and sloping posteriad, sometimes with concave anterior surfaces. Excretory pore usually at level of anterior end of procorpus. Pharyngeal gland with a large mononucleate dorsal lobe and two subventral gland lobes, usually difficult to see. Perineal pattern mostly rounded to oval, with moderately high dorsal arch that is mostly rounded and sometimes squarish and generally low, with fine, sinuous cuticle striae, which become coarser in the vicinity of perivulval region; lateral field not clearly visible. However, in some specimens the lateral fields were slightly marked. In a few specimens, the striae form two wings or shoulders ending near the lateral field, which, in this case, are made more visible by fine and small zigzag striae. Phasmids distinct, located just above the level of anus. Vulva slit in the middle of the unstriated area, almost as long as the vulva-anus distance; anus fold clearly visible, but not always present (Figs. 1i and 2q to s). Punctations and striae absent in perineum. Commonly, large egg sac occurs outside the root gall, containing up to 350–450 eggs.

Male Body vermiform, tapering anteriorly; tail rounded, with twisted posterior body portion. Lip region slightly set off from body and with a high head cap. Lip framework strong and sclerotised. Prominent slit-like amphidial openings between labial disc and lateral lips (Fig. 3e to f). In SEM view, the labial disc is slightly narrower and raised above the merged subventral and subdorsal medial lip sectors, with a centred oval prestoma into which opens a slit-like dorso-ventrally oriented stoma; lateral lips reduced to a very narrow strip, largely fused, in the middle part, with the post-labial annulus. Lip region high and lacking annulation. Stylet robust and straight, with cone and shaft broadening slightly in the distal part. Stylet knobs mostly rounded, laterally or obliquely directed, merging gradually with the base of the shaft. Lateral field consisting of four incisures with areolations along body but only few actually cross central field. Procorpus distinctly outlined, three times larger than metacorpus. Metacorpus ovoid, with a strong valve apparatus. Excretory duct curved. Excretory pore distinct and usually located four to six annuli posterior to hemizonid. Normally only one testis extending anteriorly. Spicules of variable length, arcuate and with two pores clearly visible at tip. Gubernaculum distinct. Phasmids at level of cloacal aperture and located in central lateral field, showing slit-like openings. All morphometric measurements of adult males are given in Table 1.

Second-stage juveniles Body vermiform (Figs. 1a and 2h), tapering more towards posterior than anterior end. Lip region narrower than body and slightly set off (Figs. 1b and 2i). Head cap slightly elevated. Lip framework weakly developed (Figs. 1c and 2j). Labial disc and medial lips fused. In labial disc, a stoma-like slit located in an ovoid prestoma and surrounded by six inner labial sensilla. In SEM view, the labial disc appears oval to rectangular in shape, raised above medial lips, to which it merges in a dumbbell-shaped structure. Lip region smooth and lacking annulation (Fig. 3j to k). Amphidial apertures elongated and located between labial disc and lateral lips (Fig. 3l). Body annulated from anterior end to terminus. Lateral field consisting of four incisures, with areolations along body but only few extending across field. Stylet delicate, with cone straight, narrow, sharply pointed, shaft almost

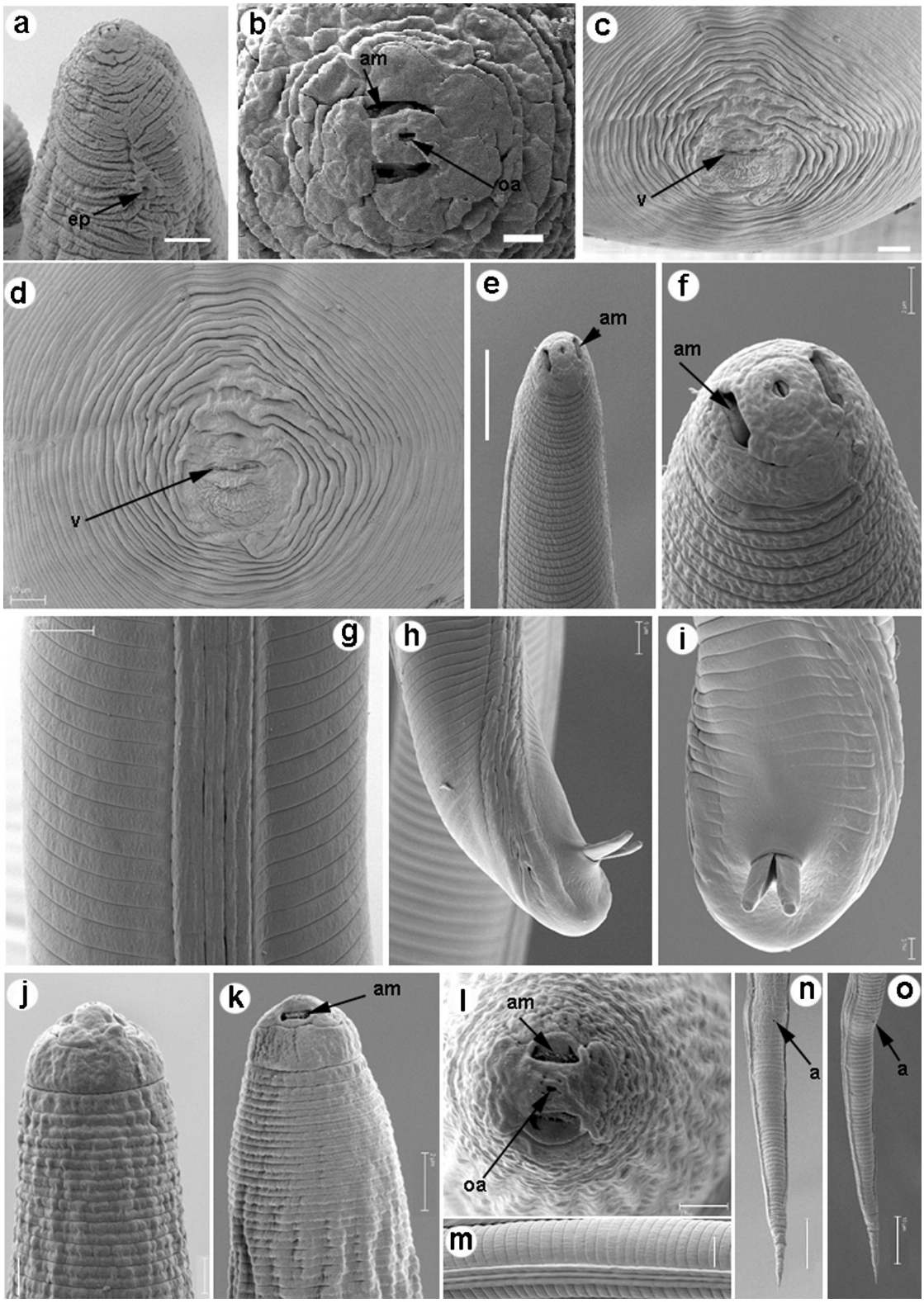
a
ep
b
am
oa
c
v
d
v
e
am
f
am
g
h
i
j
k
am
l
am
oa
m
n
a
o
a

Fig. 3 Scanning electron microscope photographs of *Meloidogyne spartelensis* n. sp. from Morocco. Female (**a-d**). **a** anterior end in lateral view showing excretory pore. **b** Lip region in *en face* view. **c-d** Perineal pattern. Male (**e-i**). **e** Anterior end in ventro-lateral view. **f** Lip region in *en face* view. **g** Lateral field at mid-body. **h-i** Tail region. Second-stage juvenile (**j-o**). **j-k** Lip region in lateral view. **l** Lip region in *en face* view. **m** Lateral field at mid-body. **n-o** Tail region. Abbreviations: a=anus; am= amphid; ep=excretory pore; oa=oral aperture; v=vulva. (Scale bars: **a**, **g**, **h**, **m**=5 μm; **b**, **j**, **l**=1 μm; **c-e**, **n**, **o**=10 μm; **f**, **i**, **k**= 2 μm;)

cylindrical, and knobs small, rounded, separate from each other, laterally directed. Pharynx with a long, cylindrical Procorpus (3.0-4.0 times length of metacorpus), round-oval metacorpus, short isthmus and rather long gland lobe, with three equally sized nuclei and overlapping intestine ventrally. Hemizonid located anterior to excretory pore, extending for *ca*. two body annuli. Excretory pore located posterior to nerve ring. Excretory duct curved and discernible when it reaches intestine. Rectum slightly dilated. Tail long, conoid, terminus usually pointed, with several constrictions in the hyaline region (Figs. 2 and 3). Tail annulation fine, regular in the proximal two third, becoming slightly coarser and irregular in the distal part. Hyaline tail terminus clearly defined and long, phasmids small, difficult to observe. All morphometric measurements carried out on second-stage juveniles are given in Table 1.

Associated host and locality

Meloidogyne spartelensis n. sp. was found in a loamy-clay soil around the roots of wild olive (*Olea europaea* subsp. *europaea* var. *sylvestris*) at Cape Spartel, near Tanger city, northern Morocco (35.790583°N; 5.924983°W, altitude 16 m).

Table 1 Morphometrics of adult males and second-stage juveniles (J2) of *Meloidogyne spartelensis* n. sp. All measurements in μm and in the format: mean±s.d. (range)*

	Males	Second stage juveniles
n	9	15
L	1497±154 (1144–1633)	451±25.1 (398–489)
Stylet	18.6±0.7 (17.5–19.5)	14.0±0.5 (13.0–14.5)
Stylet conus	9.4±0.6 (8.5–10.5)	7.7±0.5 (7.0–8.5)
Knobs width	4.5±0.6 (4.0–5.5)	2.0±0.3 (1.5–2.5)
D.G.O.	3.3±0.6 (2.5–4.0)	2.1±0.6 (1.5–3.0)
O (%)	17.6±3.1 (13.9–21.6)	15.2±4.5 (10.7–20.7)
Pharynx (to cardia)	–	127±25.1 (85–165)
Pharynx. (to end of gland lobe)	194±20.7 (167–226)	141±17.1 (109–165)
Pharyngeal overlap	–	45±8.2 (34–54)
Lip end to excretory pore	145±9.7 (133–159)	84±12.7 (60–109)
Max body diam.	33±3.2 (28–37)	15.3±1.1 (14.0-17.5)
Testis length	757±83.8 (672–894)	–
T (%)	54.5±6.4 (44.0–62.3)	–
Tail length	13.2±1.8 (10.0–16.0)	78.8±7.1 (69–93)
Anal body diam.	25.5±2.4 (23.0–28.5)	10.8±1.0 (9.5–13.5)
Tail hyaline portion (J2)	–	28.1±10.8 (19.5–46.0)
Spicules	27.5±1.8 (25.0–30.5)	–
Gubernaculum	6.9±0.3 (6.5–7.5)	–
a	42.5±2.1 (40.1–46.3)	28.9±3.1 (22.7–34.9)
b	–	3.7±0.9 (2.8–5.2)
b’	7.3±1.0 (6.4–9.1)	3.3±0.4 (2.7–3.8)
c	107.8±20.9 (75.0–141.1)	5.8±0.5 (5.0–6.4)
c’	0.5±0.1 (0.4–0.6)	7.3±0.8 (6.3–8.8)

*Abbreviations are defined in Siddiqi (2000)

Type material

Holotype female, female perineal patterns, J2 and paratype males, mounted on glass slides deposited in the authors' nematode collection at the Institute for Sustainable Agriculture, CSIC, Córdoba, Spain. Additional males and J2 paratypes were distributed to the United States Department of Agriculture Nematode Collection, Beltsville, MD, WANECO collection, Wageningen, The Netherlands (http://www.waneco.eu/), and IRD collection, Montpellier, France. Specific D2-D3, ITS, 18S-rDNA and *coxII*-16S rRNA and *coxI* of mtDNA sequences are deposited in GenBank with accession numbers KP896292-KP896293, KP896294, KP896295, KP896297, and KP997290-KP997301 respectively.

Diagnosis and relationships

Meloidogyne spartelensis n. sp. is characterized by a stylet (14.5–15.5) μm long, a perineal pattern mostly rounded to oval, with moderately high dorsal arch that is mostly rounded and sometimes squarish and generally low, excretory pore usually at level of anterior end of procorpus (EP/ST ratio=1.4–2.0), second-stage juveniles with smooth lip region, tail long, conoid, terminus pointed, with several constrictions in the hyaline region (19.5–46.0) μm long, males with stylet 17.5–19.5 μm long, and specific D2-D3, ITS, 18S-rDNA, partial *coxII*-16S rRNA and *coxI* sequences.

The female perineal pattern morphology of *M. spartelensis* n. sp. is roundish without marked lateral lines, which places it in Jepson's Group 3 (Jepson 1987). While considering the species morphology, *M. spartelensis* n. sp. is related to the "graminis-group" studied by Jepson (1987), it is morphometrically closer to *M. kralli* (Jepson 1983). Females differ by EP/ST (1.4–2.0 vs. 2.0–3.0 in *M. kralli*). Juveniles were smaller b ratio (3.7 *vs* 6.5), longer stylet (13.0–14.5 *vs* 10.5–11.5 μm), and shorter DGO (2.1 *vs* 4.1). Males were longer (1497 *vs* 1076 μm), higher a ratio (42.5 *vs* 31.7), shorter DGO (3.3 *vs* 4.4) and longer distance from anterior end to excretory pore (145 *vs* 127.4). Partial 18S from *M. kralli* (KJ636370) is also different to *M. spartelensis* n. sp. in 3 % differences (24 nucleotides in difference).

Meloidogyne spartelensis n. sp. is also similar to *M. dunensis*, from which it differs mainly in morphology of female perineal patterns (lateral field clear visible on *M. dunensis*). Juvenile stylet is longer (13.0–14.5 *vs* 11.0–12.5 μm) and as its hyaline part of tail (19.5–46.0 *vs* 9.5–16.5 μm). In males, c ratio (107.8 *vs* 280.6) and spicules (25.0–30.5 *vs* 29.0–38.0 μm) were smaller. The new species is also morphologically close to *M. sewelli*, from which it differs mainly in higher female EP/ST ratio (1.4–2.0 *vs* 1.2), longer length of J2 stylet (13.0–14.5 vs. 11.0–12.0 μm), and in shorter length of male gubernaculum (6.5–7.5 *vs* 8.0–9.0 μm) and shorter DGO (2.5–4.0 *vs* 5.0–6.0). D2-D3, ITS and partial 18S sequences from *M. dunensis* (EF612713, EF612711 and EF612712, respectively) are also different to *M. spartelensis* n. sp. in 7 % differences (51 nucleotides), 6 % differences (25 nucleotides), and 2 % differences (16 nucleotides), respectively. *Meloidogyne spartelensis* n. sp. can also be compared with several other *Meloidogyne* species commonly infecting woody plants, such as *M. arenaria*, *M. baetica*, *M. hispanica*, *M. incognita* and *M. javanica*. Their main comparative diagnostic characters, useful to a rapid and easy identification, are summarized in Table 2. *Meloidogyne spartelensis* n. sp. also differs markedly from the other known European root-knot nematode species (Karssen and van Hoenselaar 1998; Karssen 2002; Castillo et al. 2003b).

In addition, *M. spartelensis* sp. n. differs from related species in Est and Mdh phenotypes, as well as sequences of the ITS1-5·8S-ITS2 region, the small subunit 18S rDNA, the D2-D3 fragment of the 28S gene of rDNA, the *coxII*-16S rRNA, and *coxI* gene sequences (see below).

Isozyme analysis and molecular characterization

The isozyme electrophoretic analysis of five-specimen groups of young egg-laying females of *M. spartelensis* n. sp. revealed one strong Est band (Rm=42.65) after prolonged staining (Fig. 4a) and one N1b Mdh band (Fig. 4b) that did not occur in the Est and Mdh phenotypes of *M. javanica*, which showed J3 and N1 phenotypes, respectively (Fig. 4a and b) or in other Est and Mdh phenotypes previously identified for other *Meloidogyne* spp. Malate dehydrogenase phenotype of *M. spartelensis* n. sp. clearly differs from that of *M. kralli* (with N1c bands) (Karssen 2002), showing a lower unique band for *M. spartelensis* n. sp in comparison to *M. javanica* and those of *M. dunensis* (with a weak VS1 and N1c bands, respectively, Table 2), with a

Morphological and morphometric differences among *Meloidogyne* species closely related to *Meloidogyne spartelensis* n. sp. and parasite species to olive[a, b]

		spartelensis n. sp.	*arenaria*	*baetica*	*dunensis*	*incognita*	*javanica*	*kralli*	*lusitanica*	*sewelli*
Female										
Stylet length		15.1 (14.5–15.5)	15.5 (14.4–15.8)	17.5 (17–19)	14 (13–16)	14 (13–16)	17.0 (14.0–18.0)	18.2 (17.6–19.0)	17 (16–19)	14.5 (14.0–15.0)
Knobs shape		oval and sloping posteriorly, sometimes with concave anterior surfaces	rounded and backwardly directed	ovoid, sloping backwards	rounded and/or sloping backwards	rounded or drawn out laterally	rounded	knobs set off from shaft, rounded and transversely ovoid	ovoid and backwardly directed	knobs small, rounded
EP/ST ratio		1.5 (1.4–2.0)	2.4	0.7 (0.5–0.8)	1.6 (1.2–1.8)	1.4	–	(2.0–3.0)	2.6 (1.6–3.8)	1.2
Perineal pattern		rounded, with numerous fine sinuous dorsal and smooth ventral striae, with lateral fields usually not visible	round to oval with dorsal arch low, striae fairly widely separated and lateral field usually marked by some forked and broken striae	distinct inner striae forming two distinct longitudinal bands, extending throughout the perineum to just below the vulva	rounded to oval with numerous fine dorsal and ventral striae, lateral field clear visible	striae closely spaced, very wavy to zig-zag, dorsal arch high	striae interrupted laterally by conspicuous double incisures edging lateral ridges	Circular to ovoid with fine striae, lateral field faintly visible.	striking, trapezoid with coarse striae and medium to high dorsal arch	rounded dorsal arch and many discontinuous, closely spaced striae
Isozyme[c] phenotype	Est	VS1	A1,A2,A3	VS1	VS1	I1	J3	–	A1	–
	Mdh	N1b	N1	N1c	N1c	N1	N1	N1c	P3	–
Second-stage juvenile										
Body length		451 (398–489)	(450–490) 738 (510–1.012)	403 (394 to 422)	446 (417–483)	371 (337–403)	417 (387–459)	439 (408–476)	450 (390–515)	505 (460–540)
Stylet length		14.0 (13.0–14.5)	11.6 (11.1–12.6)	13.5 (13–14)	11.5 (11.0–12.5)	10.5 (9.6–11.7)	10.4 (9.4–11.4)	10.8 (10.5–11.5)	14.2 (13–16)	(11.0–12.0)
Hemizonid position		2–3 annuli to EP	anterior, not adjacent to EP	2–3 annuli anterior to EP	anterior, adjacent to EP	just anterior to EP	immediately anterior to EP	anterior to EP	one or two annuli anterior to EP	–
Tail length		78.8 (69–93)	55.8 (52.2–59.9)	50 (47–54)	68 (54–82)	48.7 (45–52)	49(36–56)	68.1 (61.0–78.0)	44 (39–50)	76 (70–82)
Tail hyaline portion		28.1 (19.5–46.0)	14.8 (10.8–19.8)	12 (10–13)	14.0 (9.5–16.5)	8.9 (6.3–13.5)	13.7 (9.8–18.0)	17.4 (14.5–21.0)	12 (10–14)	12.0 (9.0–13.5)
Male										
Stylet length		18.6 (17.5–19.5)	21.6 (20.7–23.4)	17 (16–19)	20 (16–22)	24.8 (24.3–26.1)	20.3 (18.9–23.4)	18.8 (18.0–20.0)	24.5 (21–27)	19.0 (18.0–20.0)
Knobs shape		rounded, laterally or obliquely directed, merging gradually with the base of the shaft	smoothly rounded to stylet	rounded and sloping backwards	relatively small, rounded, set off	rounded with flat, concave or toothed anterior margins	low and wide, often anteriorly indented, and set off from the shaft	knobs set off from shaft, rounded and somewhat transversely ovoid	elongate, pear shaped, slightly set off from shaft	rounded
Spicules		27.5 (25.0–30.5)	25.7 (31–34)	27 (24–36)	35.3 (29–38.1)	35 (29–40)	29.5 (22.9–35.3)	26.3 (22.5–28.0)	37.9 (32.0–44.5)	29 (28.0–30.0)
Gubernaculum		6.9 (6.5–7.5)	8.2 (7.2–9.4)	12 (10–14)	8.5 (6.0–10.5)	11.2 (9.4–13.7)	8.0 (5.7–10.1)	–	10.2 (8.5–12.0)	(8.0–9.0)

[a] All measurements are in μm unless otherwise stated

[b] Measurements in Abrantes and Santos 1991; Castillo et al. 2003b; Jepson 1983, 1987; Palomares-Rius et al. 2007

[c] Isozyme phenotypes used are defined by Esbenshade and Triantaphyllou (1985)

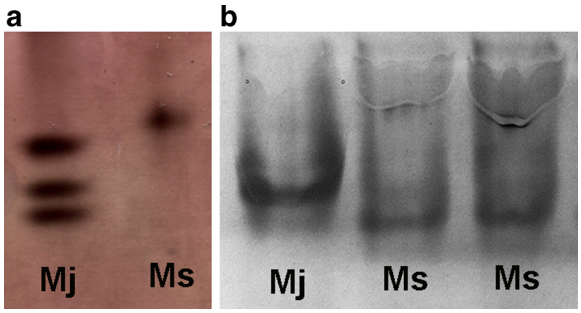

Fig. 4 Esterase (**a**) and malate dehydrogenase (**b**) phenotype electrophoresis patterns of protein homogenates from five young, egg-laying females of *Meloidogyne spartelensis* n. sp. from Morocco (Ms), and five young, egg-laying females of *M. javanica* reference population (Mj)

lower esterase band and higher Mdh band, respectively, taking as reference *M. javanica* for *M. spartelensis* n. sp.

Amplification of the 18S, ITS1-5.8S-ITS2, D2-D3 region of 28S rDNA, and partial *coxII*-16S rRNA and *coxI* mtDNA from *M. spartelensis* n. sp. yielded single fragments of approximately 900, 700, 840, 500 and 400 bp respectively. The partial D2-D3, ITS1-5.8S-ITS2, 18S, and partial *coxII*-16S rRNA sequences of *M. spartelensis* n. sp. were clearly different from that present in the GenBank database. Substantial sequence divergence for D2-D3 region of 28S (7 % against *M. dunensis*, (EF612712)), ITS1-5.8S-ITS2 (11 % against *M. hispanica* Hirschmann 1986 (JX885742)), partial 18S (1 % against *M. ardenensis* Santos, 1968 (AY593894)), and partial *coxII*-16S rRNA (19 % against *M. hapla*, AY757889) sequences for the new species distinguish *M. spartelensis* n. sp. from other studied root-knot nematodes and support its separate specific status. *CoxI* gene sequences from *M. spartelensis* n. sp. (KP997290- KP997301) showed a similarity of 89 % with *M. hapla* (JX683718 and AY268113) and 86 % with *M. javanica* (KP202352), *M. arenaria* (KP202350) and *M. incognita* (KJ476151). Intraspecific variability for *COI* gene was of 99.6 % (1 nucleotide in 322).

Phylogenetic analysis (BI and ML) of *M. spartelensis* n. sp. based on D2-D3 expansion segments of 28S rDNA of a multiple edited alignment including 56 sequences and 765 bp showed one clade clearly separated and supported (Fig. 5). The phylogenetic analysis showed well supported groups at major and terminal clades in both analyses. The phylogenetic tree resolved a major clade excluding *M. mali* Itoh et al. 1969 (KF880399 and KF880400), *M. camelliae* Golden 1979 (KF542870), *M. ichinohei* Araki 1992 (EF029862), *M. artiellia* Franklin 1961 (AY150369) and *M. baetica* (AY150367). *Meloidogyne spartelensis* n. sp. is closely related to *M. dunensis* (EF612712) and *M. silvestris* Castillo et al. 2009 (EU570214) and in a higher clade level with *M. hapla* (KJ645433 and KJ598136).

Phylogenetic analysis (BI and ML) of *M. spartelensis* n. sp. based on ITS sequences of a multiple edited alignment including 71 sequences and 681 total characters showed one clade clearly separated and supported (Fig. 6). Similarly to D2-D3 expansion segments of 28S rDNA phylogeny *M. artiellia* (KC545880, JX393299 and AF248478), *M. baetica* (AY150366), *M. camelliae* (KF542872, JX912885 and KF542871), *M. mali* (JX978229) and *M. panyuensis* Liao et al. 2005 (AY394719) were not included in this major and well supported clade. *Meloidogyne spartelensis* n. sp. formed a well-supported clade with *M. dunensis* (EF612711).

Phylogenetic analysis (BI and ML) of *M. spartelensis* n. sp. based on partial 18S sequences of a multiple edited alignment including 76 sequences and 1641 bp showed several nested clades clearly separated and supported (Fig. 7). A major clade including 62 sequences was well supported while *M. mali* (KJ636400, KC875395, KF895400 and JX978225) occupied a basal position to this clade. *Meloidogyne artiellia* (KC875391 and KC875392) and *M. baetica* (KP896296) formed a well-supported clade nested to the clades explained before. Finally, *M. ichinohei* (KJ636350, KC875386 and KJ636349), *M. camelliae* (JX912884) and *M. coffeicola* Lordello & Zamith 1960 (HE667739) formed a well-supported basal clade to the other species. *Meloidogyne spartelensis* n. sp. was related to *M. microtyla* Lordello & Zamith 1960 (AF442198), and *M. ardenensis* (AY593894) in a moderately supported clade that also includes *M. graminis* (Sledge & Golden 1964) Whitehead 1968 (JN241856) in a moderately supported clade.

Phylogenetic analysis (BI and ML) of *M. spartelensis* n. sp. based on the partial *coxII*-16S rRNA of a multiple edited alignment including 62 sequences with 1633 bp in length showed two moderate supported clades (Fig. 8). One clade contained the majority of the species while the other was formed by *M. camelliae* (JX912887) and *M. mali* (KC112913). In the main clade, *Meloidogyne spartelensis* n. sp. is sister to two well-supported subclades: the first including *M. arenaria*, *M. thailandica* Handoo et al. 2005, *M. morocciensis*

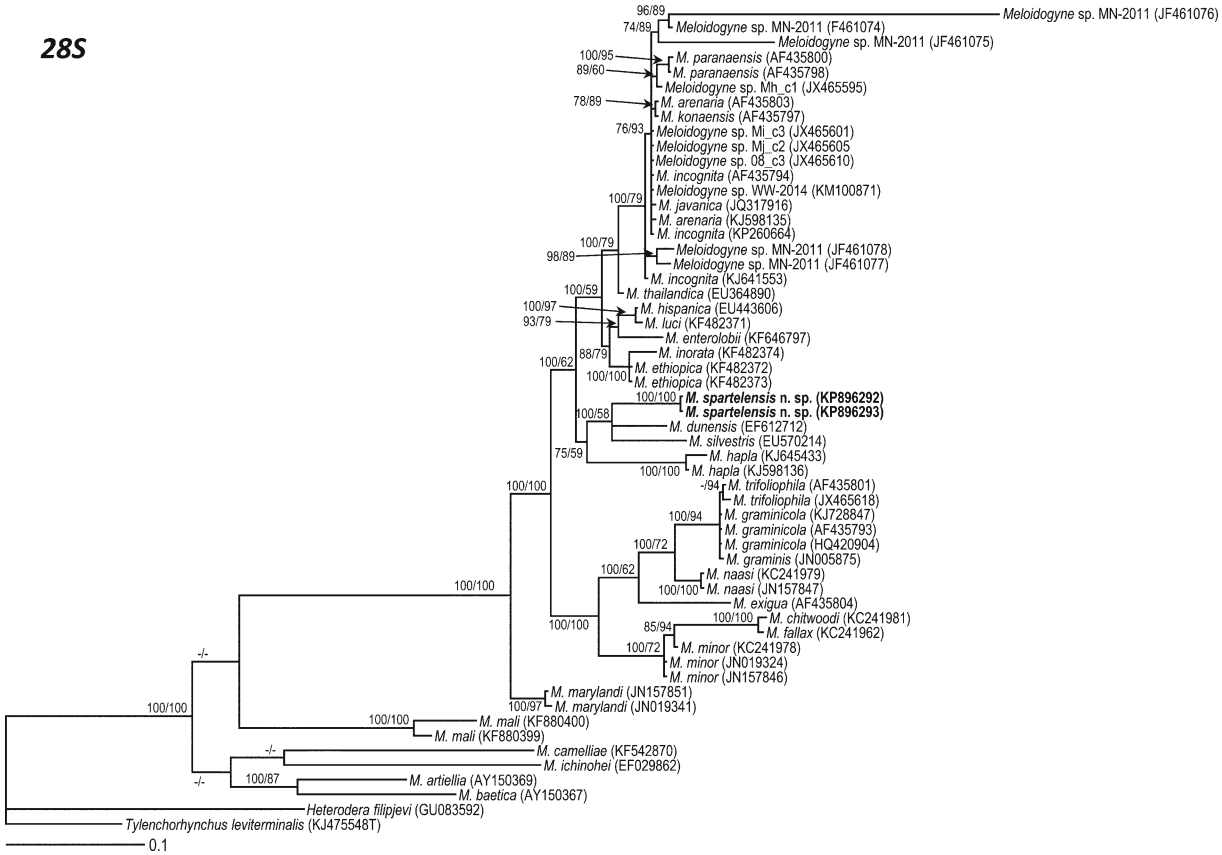

Fig. 5 Phylogenetic relationships within *Meloidogyne* species. Bayesian 50 % majority rule consensus trees as inferred from D2 and D3 expansion segments of 28S rDNA sequences alignments under the GTR+I+G model. Posterior probabilities more than 65 % are given for appropriate clades; bootstrap values greater than 50 % are given on appropriate clades in ML analysis. Newly obtained sequences in this study are in bold font

Handoo et al. 2005, *M. javanica*, *M. incognita*, *M. floridensis* Handoo et al. 2004, *M. ethiopica* Whitehead 1968, *M. paranaensis* Carneiro et al. 1996, *M. arabicida* López & Salazar 1989, *M. enterolobii* Yang & Eisenback 1983, *M.* cf. *haplanaria* Eisenback et al. 2003 plus other species not identified, and the second including *M. hapla* and *M. partytila* Kleynhans, 1986 in the other clade.

Discussion

The primary objective of this study was to identify and molecularly characterize a species of *Meloidogyne* detected in wild olive soils in northern Morocco. However, this species was not related morphologically to the other species associated with olive such as *M. arenaria*, *M. artiellia*, *M. baetica*, *M. hapla*, *M. incognita*, *M. javanica*, and *M. lusitanica* (Castillo et al. 2010; Ali et al. 2014) (see Table 2). The main character in its juveniles associated with the long tail and hyaline region indicates this species would be associated with the "graminis" group (Jepson 1987). However, its associated host plant (wild olive) is different to the main species in this group (mainly associated to monocotyledon plants). Other plants such as arundo canes, lentisc, *Phillyrea*, Mimosaceae schrubs, maritime pine and eucalyptus trees, etc. were also detected in the same site.

It also differs phylogenetically from this "graminis" group of species but is related to *M. dunensis* and *M. silvestris* associated in the Iberian peninsula with dicotyledonous plants and with woody plants respectively (Palomares-Rius et al. 2007; Castillo et al. 2009). The reproduction on tomato of this new species also

Fig. 6 Phylogenetic relationships within *Meloidogyne* species. Bayesian 50 % majority rule consensus trees as inferred from ITS rDNA gene sequence alignment under the GTR+G model. Posterior probabilities more than 65 % are given for appropriate clades (in bold letters); bootstrap values greater than 50 % are given on appropriate clades in ML analysis. Newly obtained sequence in this study are in bold font

expands its host-range, as for the polyphagous root-knot nematode species *M. incognita*, *M. javanica* and *M. arenaria* that are able to infect olive and other hosts. However, the other group of species that parasite olive (*M. baetica* and *M. lusitanica*) have a very restricted host-range and limited prevalence (El-Borai and Duncan 2005). Despite no *M. spartelensis* n. sp. surviving on olive cv. Picholine du Languedoc (may be due to cultivar incompatibility or low initial inoculum density), pathogenicity experiments should be carried out with *M. spartelensis* n. sp. in order to verify the olive host suitability.

Phylogenetic analysis of the used molecular markers (D2-D3 region, ITS, partial 18S, partial *coxII*-16S rRNA and *coxI* sequences) demonstrates that *M. spartelensis* n. sp. is different to the other species with molecular markers in GenBank. It is clearly phylogenetically related to *M. dunensis*, found in Spain (Cullera, Valencia Province) with sea rocket (*Cakile maritima* Scop.) in coastal dunes. Both species are able to infect tomato and possess long tails with similar morphological traits. Probably both species evolved from the same ancestor species. This species is also related to *M. silvestris* with only a woody host known (*Ilex aquifolium* L.) and also described in the Iberian Peninsula. These species group seems to be related to a diversification process in the Mediterranean basin with restricted areas of distribution in natural

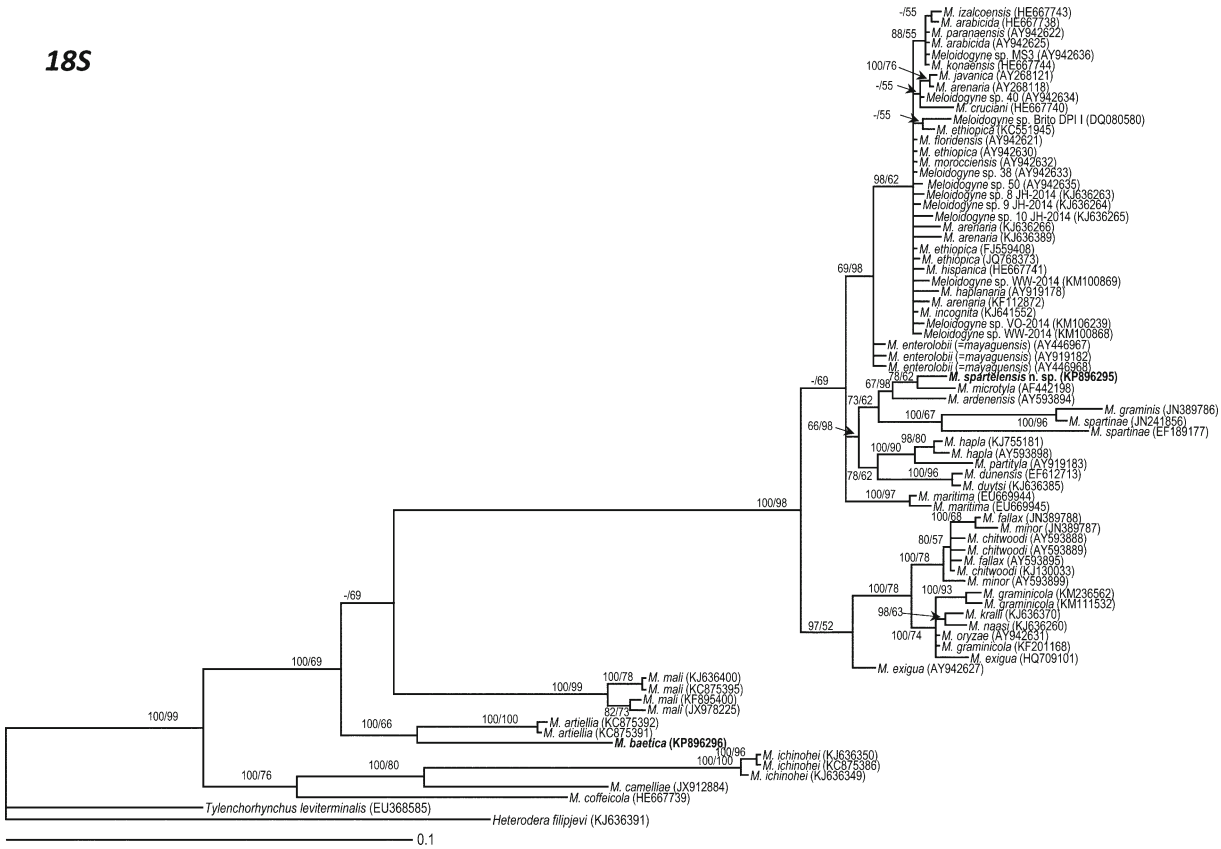

Fig. 7 Phylogenetic relationships within *Meloidogyne* species. Bayesian 50 % majority rule consensus trees as inferred from partial 18S gene sequence alignment under the GTR+I+G model. Posterior probabilities more than 65 % are given for appropriate clades (in bold letters); bootstrap values greater than 50 % are given on appropriate clades in ML analysis. Newly obtained sequences in this study are in bold font

environments. This could be partially due to long persistence of *Meloidogyne* spp. in isolated regions (i.e., allopatric speciation), in particular during last glacial maximum. Indeed, the place where *M. spartelensis* n. sp. was detected belongs to the Rif-Mountain plant-refuge area (Médail and Diadema 2009) and to the Gibraltar strait biodiversity hot-spot (Rodriguez-Sanchez et al. 2008). In this specific area, wild olive consists in an ancestral wild gene pool with unique haplotypes (Besnard et al. 2013) supporting refuge conditions. The ability of some *Meloidogyne* species to infect olive tree seems to be acquired in several events in their evolution and not from a unique event, because species with restricted ability to infect other hosts, as *M. baetica* are related phylogenetically nor with them and nor the other group of highly polyphagous species (*M. incognita*, *M. javanica* and *M. arenaria*). *Meloidogyne lusitanica* did not have molecular markers in order to extend this supposition. However, this hypothesis is not completely tested with the lack of host test for *M. baetica*, *M. lusitanica* and *M. spartelensis* n. sp. Phylogenetic trees with the markers used showed the ancestry of certain species in the different markers studied, i.e., *M. mali*, *M. camelliae*, *M. ichinohei*, *M. artiellia*, *M. panyuensis*, *M. coffeicola* and *M. baetica*. This result is similar to other phylogenetic analysis with a more limited number of *Meloidogyne* spp. (Adams et al. 2009).

Meloidogyne spartelensis n. sp. also differs from Est and Mdh isozyme electrophoretic patterns to the other species closely related morphologically and specific to olive parasitism. Differences in the number of bands and their gel position give us the possibility to differentiate

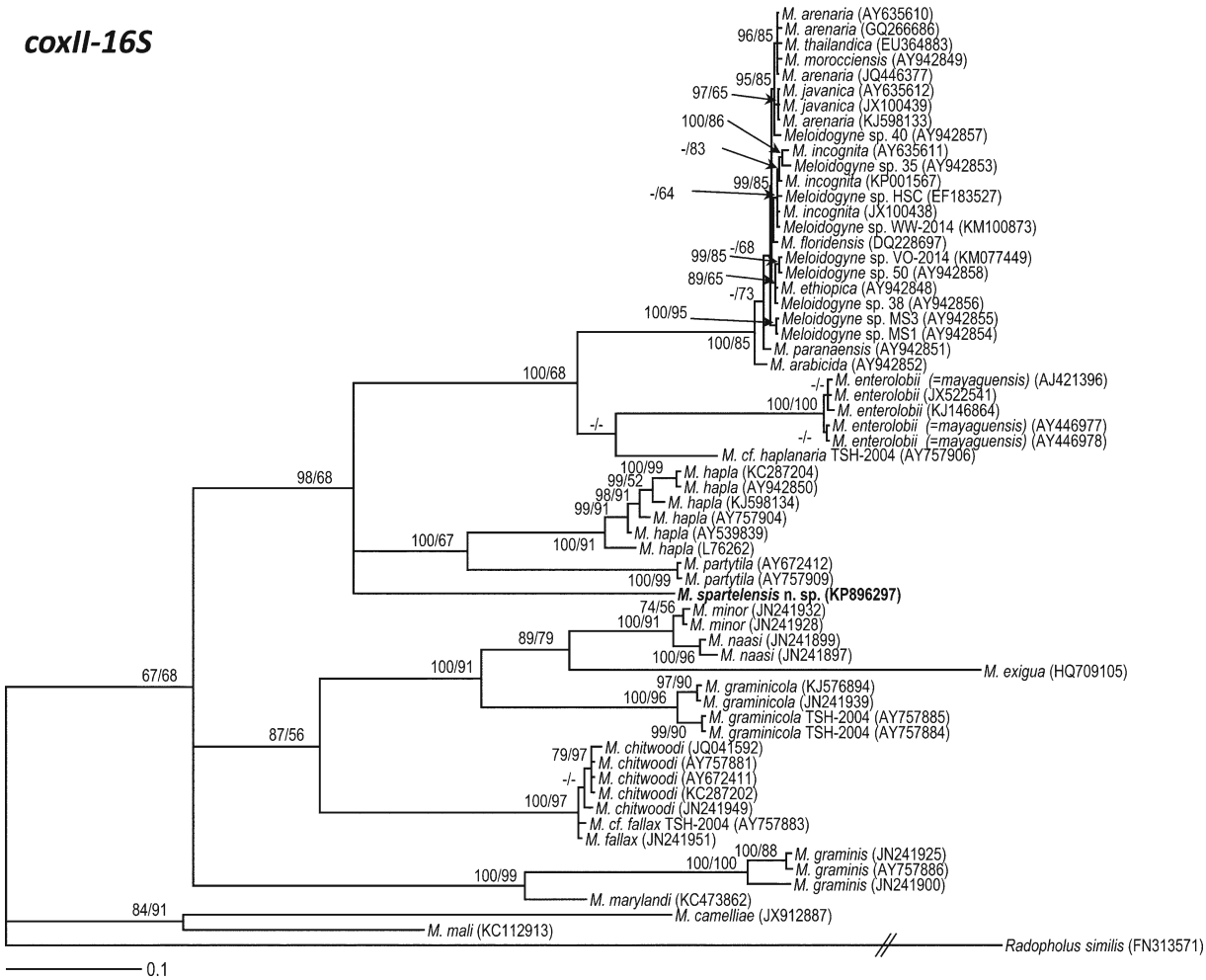

Fig. 8 Phylogenetic relationships within *Meloidogyne species*. Bayesian 50 % majority rule consensus trees as inferred from partial *coxII-16S* rRNA genes sequences alignment under the GTR+I+G model. Posterior probabilities more than 65 % are given for appropriate clades (in bold letters); bootstrap values greater than 50 % are given on appropriate clades in ML analysis. Newly obtained sequence in this study are in bold font

it. The analysis of isozyme electrophoretic patterns, in particular Est and Mdh, as well as several molecular approaches have been proved to be a valuable tool for precise identification of *Meloidogyne* species (Flores Romero and Navas 2005; Blok and Powers 2009). This accurate species description with molecular markers associated to the type population (D2-D3 region, ITS, partial 18S and partial *coxII*-16S rRNA; *coxI* of mtDNA) will provide accurate markers for the unequivocal species identification and monitoring the possibility of expansion or identification in other untested areas.

In summary, present study establishes the importance of using polyphasic identification highlighting the time consuming aspect and difficulty of a correct identification at species level within the *Meloidogyne* spp. and describes a new root-knot nematode associated with wild olive in the Mediterranean Basin area.

Acknowledgments This research was supported by grant KBBE219262 ArimNET_ERANET FP7 2012–2015 Project PESTOLIVE 'Contribution of olive history for the management of soilborne parasites in the Mediterranean basin' from Agence Nationale de la Recherche (ANR, France) and Instituto Nacional de Investigación y Tecnología Agraria y Alimentaria (INIA, Spain), grant Long-Term Mission Program from Institut de Recherche pour le Développement (IRD, France), PhD grant from Tishreen University (Syrian Arab Republic), grant ANR-10-LABX-41 from LABEX TULIP (France), grant AGR-136 from 'Consejería de Economía, Innvovación y Ciencia' from Junta de Andalucía, and Union Europea, Fondo Europeo de Desarrollo regional, "Una manera de hacer Europa". The authors thank J.

Martín Barbarroja and G. León Ropero from IAS-CSIC for the excellent technical assistance.

References

Abolafia, J., Liébanas, G., & Peña-Santiago, R. (2002). Nematodes of the order rhabditida from andalucia oriental, Spain. The subgenus pseudacrobeles Steiner 1938, with description of a new species. *Journal of Nematode Morphology and Systematics, 4*, 137–154.

Abrantes, I. M., & Santos, S. (1991). *Meloidogyne lusitanica* n. sp. (Nematoda: Meloidogynidae), a root-knot nematode parasitizing olive tree (*Olea europaea* L.). *Journal of Nematology, 23*, 210–224.

Adam, M. A. M., Phillips, M. S., & Blok, V. C. (2007). Molecular diagnostic key for identification of single juveniles of seven common and economically important species of root-knot nematode (*Meloidogyne* spp). *Plant Pathology, 56*, 190–197.

Adams, B. J., Dillman, A. R., & Finlinson, C. (2009). Molecular taxonomy and phylogeny. In R. N. Perry, M. Moens, & J. L. Starr (Eds.), *Root-knot nematodes* (pp. 55–97). Wallingford, UK: CABI.

Ali, N., Chapuis, E., Tavoillot, J., & Mateille, T. (2014). Plant-parasitic nematodes associated with olive tree (*Olea europaea* L.) with a focus on the Mediterranean basin: a review. *Comptes Rendus Biologies, 337*, 423–442.

Araki, M. (1992). Description of Meloidogyne ichinohei n. sp. (Nematoda: Meloidogynidae) from Iris Iaevigata in Japan. *Japanese Journal of Nematology, 22*, 11–20.

Besnard, G., Khadari, B., Navascues, M., Fernandez-Mazuecos, M., El Bakkali, A., Arrigo, N., Baali-Cherif, D., Brunini-Bronzini de Caraffa, V., Santoni, S., Vargas, P., & Savolainen, V. (2013). The complex history of the olive tree: from late quaternary diversification of Mediterranean lineages to primary domestication in the Northern Levant. *Proceedings of the Royal Society B, 280*, 20122833.

Blok, V. C., & Powers, T. O. (2009). Biochemical and molecular identification. In R. N. Perry, M. Moens, & J. L. Starr (Eds.), *Root-knot nematodes* (pp. 55–97). Wallingford, UK: CABI.

Carneiro, R. M. D. G., Carneiro, R. G., Abrantes, I. M. O., Santos, M. S. N. A., & Almeida, M. R. A. (1996). Meloidogyne paranaensis n. sp. (Nemata: Meloidogynidae), a root-knot nematode parasitizing coffee in Brazil. *Journal of Nematology, 28*, 177–189.

Castillo, P., Vovlas, N., & Troccoli, A. (2003a). The reniform nematode *Rotylenchulus macrosoma* infecting olive in southern Spain. *Nematology, 5*, 23–29.

Castillo, P., Vovlas, N., Subbotin, S., & Troccoli, A. (2003b). A new root-knot nematode, *Meloidogyne baetica* n. sp. (Nematoda: Heteroderidae), parasitizing wild olive in Southern Spain. *Phytopathology, 93*, 1093–1102.

Castillo, P., Vovlas, N., Troccoli, N., Liébanas, G., Palomares Rius, J. E., & Landa, B. B. (2009). A new root-knot nematode, *Meloidogyne silvestris* n. sp. (Nematoda: Meloidogynidae), parasitizing European holly in Northern Spain. *Plant Pathology, 58*, 606–619.

Castillo, P., Nico, A. I., Navas-Cortes, J. A., Landa, B. B., Jiménez-Díaz, R. M., & Vovlas, N. (2010). Plant-Parasitic nematodes attacking olive trees and their management. *Plant Disease, 94*, 148–162.

Chitwood, B. G. (1949). Root-knot nematodes – Part 1. A revision of the genus Meloidogyne Goeldi, 1887. *Proceedings of the Helminthological Society of Washington, 16*, 90–104.

Coolen, W. A. (1979). Methods for extraction of *Meloidogyne* spp. and other nematodes from roots and soil. In F. Lamberti & C. E. Taylor (Eds.), *Root-knot nematodes (Meloidogyne species). systematics, biology and control* (pp. 317–329). New York, NY, USA: Academic.

Darriba, D., Taboada, G. L., Doallo, R., & Posada, D. (2012). jModelTest 2: more models, new heuristics and parallel computing. *Nature Methods, 9*, 772.

De Ley, I. T., Karssen, G., De Ley, P., Vierstraete, A., Waeyenberge, L., Moens, M., & Vanfleteren, J. (1999). Phylogenetic analyses of internal transcribed spacer region sequences within *Meloidogyne. Journal of Nematology, 31*, 530–531.

Eisenback, J. D., Bernard, E. C., STARR, J. L., Lee, T. A., & Tomaszewski, E. K. (2003). Meloidogyne haplanaria n. sp. (Nematoda: Meloidogynidae), a root-knot nematode parasitizing peanut in Texas. *Journal of Nematology, 35*, 395–403.

El-Borai, F. E., & Duncan, L. W. (2005). Nematode parasites of subtropical and tropical fruit tree crops. In M. Luc, R. A. Sikora, & J. Bridge (Eds.), *Plant parasitic nematodes in subtropical and tropical agriculture* (pp. 467–492). Wallingford, UK: CABI.

Esbenshade, P. R., & Triantaphyllou, A. C. (1985). Use of enzyme phenotypes for identification of *Meloidogyne* species. *Journal of Nematology, 17*, 6–20.

Flores Romero, P., & Navas, A. (2005). Enhancing taxonomic resolution: distribution dependent genetic diversity in populations of *Meloidogyne. Nematology, 7*, 517–530.

Franklin, M. T. (1961). A British root-knot nematode, Meloidogyne artiella n.sp. *Journal of Helminthology*, R.T. Leiper Supplement, 85–92.

Gamel, S., Huchet, E., Roux-Nio, A. C., & Anthoine, G. (2014). Assessment of PCR-based tools for the specific identification of some temperate *Meloidogyne* species including *M. chitwoodi*, *M. fallax* and *M. minor. European Journal of Plant Pathology, 138*, 807–817.

Hall, T. A. (1999). BioEdit: a user-friendly biological sequence alignment editor and analysis program for windows 95/98/NT. *Nucleic Acids Symposium Series, 41*, 95–98.

Handoo, Z. A., Nyczepir, A. P., Esmenjaud, D., Van der Beek, J. G., Castagnone-Sereno, P., Carta, L. K., Skantar, A. M., & Higgins, J. A. (2004). Morphological, molecular, and differential-host characterization of Meloidogyne floridensis n.sp. (Nematoda: Meloidogynidae), a root-knot nematode parasitizing peach in Florida. *Journal of Nematology, 36*, 20–35.

Handoo, Z. A., Skantar, A. M., Carta, L. K., & Erbe, E. F. (2005). Morphological and molecular characterization of a new root-knot nematode, Meloidogyne thailandica n. sp. (Nematoda: Meloidogynidae), parasitizing ginger (Zingiber sp.). *Journal of Nematology, 37*, 343–353.

Hartman, K. M., & Sasser, J. N. (1985). Identification of *Meloidogyne* species on the basis of differential host test and perineal pattern morphology. In K. R. Barker, C. C. Carter, & J. N. Sasser (Eds.), *An advanced treatise on Meloidogyne* (Methodology, Vol. II, pp. 69–77). Raleigh, USA: NCSU Graphics.

Hussey, R. S., & Barker, K. R. (1973). A comparison of methods of collecting inocula of *Meloidogyne* spp., including a new technique. *Plant Disease Reporter, 57*, 1025–1028.

Itoh, Y., Ohshima, Y., & Ichinohe, M. (1969). A root-knot nematode, Meloidogyne mali n. sp. on appletree from Japan (Tylenchida: Heteroderidae). *Applied Entomology and Zoology, 4*, 194–202.

Jepson, S. B. (1983). *Meloidogyne kralli* n. sp. (Nematoda: Meloidogynidae) a root-knot nematode parasitizing sedge (*Carex acuta* L.). *Révue de Nématologie, 6*, 239–245.

Jepson, S. B. (1987). *Identification of root-knot nematodes (Meloidogyne species)*. Wallingford, UK: CABI.

Karssen, G. (2002). *The plant-parasitic nematode genus Meloidogyne Göldi, 1892 (Tylenchida) in Europe*. Leiden, The Netherlands: BRILL.

Karssen, G., & Van Hoenselaar, T. (1998). Revision of the genus *Meloidogyne* Göldi, 1892 (Nematoda: Heteroderidae) in Europe. *Nematologica, 44*, 713–788.

Katoh, K., Misawa, K., Kuma, K., & Miyata, T. (2002). MAFFT: a novel method for rapid multiple sequence alignment based on fast Fourier transform. *Nucleic Acids Research, 30*, 3059–3066.

Kleynhans, K. P. N. (1986). Meloidogyne partityla sp. nov. from pecan nut [Carya illinoensis (Wangenh.) C. Koch] in the Transvaal Lowveld (Nematoda: Meloidogynidae). *Phytophylactica, 18*, 103–106.

Kofoid, C. A., & White, W. A. (1919). A new nematode infection of man. *Journal of the American Medical Association, 72*, 567–569.

Lazarova, S. S., Malloch, G., Oliveira, C. M. G., Hübschen, J., & Neilson, R. (2006). Ribosomal and mitochondrial DNA analyses of *Xiphinema americanum*-group populations. *Journal of Nematology, 38*, 404–410.

Liao, J., Yang, W., Feng, Z., & Karssen, G. (2005). Description of *Meloidogyne panyuensis* sp. n. (Nematoda: Meloidogynidae), parasitic on peanut (*Arachis hypogaea* L.) in China. *Russian Journal of Nematology, 13*, 107–114.

López, R., & Salazar, L. (1989). Meloidogyne arabicida sp. n. (Nemata: Heteroderidae) native of Costa Rica: a new and severe pathogen of coffee. *Turrialba, 39*, 313–323.

Lordello, L. G. E., & Zamith, A. P. L. (1960). Meloidogyne coffeicola sp. n., a pest of coffee trees in the state of Parana, Brazil (Nematoda, Heteroderidae). *Revista Brasileira de Biologia, 20*, 375–379.

Médail, F., & Diadema, K. (2009). Glacial refugia influence plant diversity patterns in the Mediterranean Basin. *Journal of Biogeography, 36*, 1333–1345.

Moens, M., Perry, R. N., & Starr, J. L. (2010). *Meloidogyne* species–a diverse group of novel and important plant parasites. In M. Moens, R. N. Perry, & J. L. Starr (Eds.), *Root-knot nematodes* (pp. 1–17). Wallingford, UK: CAB International.

Mulvey, R. H., & Anderson, R. V. (1980). Description and relationships of a new root-knot nematode, *Meloidogyne sewelli* n. sp. (Nematoda: Meloidogynidae) from Canada and a new host record for the genus. *Canadian Journal of Zoology, 58*, 1551–1556.

Nico, A. I., Rapoport, H. F., Jiménez-Díaz, R. M., & Castillo, P. (2002). Incidence and population density of plant-parasitic nematodes associated with olive planting stocks at nurseries in southern Spain. *Plant Disease, 86*, 1075–1079.

Page, R. D. (1996). TreeView: an application to display phylogenetic trees on personal computers. *Computer Applications in the Biosciences, 12*, 357–358.

Palomares-Rius, J. E., Vovlas, N., Troccoli, A., Liébanas, G., Landa, B. B., & Castillo, P. (2007). A new root-knot nematode parasitizing sea rocket from Spanish Mediterranean coastal dunes: *Meloidogyne dunensis* n. sp. (Nematoda: Meloidogynidae). *Journal of Nematology, 39*, 190–202.

Palomares-Rius, J., Guesmi, I., Horrigue-Raouani, N., Cantalapiedra-Navarrete, C., Liébanas, G., & Castillo, P. (2014). Morphological and molecular characterisation of *Pratylenchus oleae* n. sp. (Nematoda: Pratylenchidae) parasitizing wild and cultivated olives in Spain and Tunisia. *European Journal of Plant Pathology, 140*, 53–67.

Powers, T. O., & Harris, T. S. (1993). A polymerase chain reaction method for identification of five major *Meloidogyne* species. *Journal of Nematology, 25*, 1–6.

Rodriguez-Sanchez, F., Perez-Barrales, R., Ojeda, F., Vargas, P., & Arroyo, J. (2008). The strait of Gibraltar as a melting pot for plant biodiversity. *Quaternary Science Reviews, 27*, 2100–2117.

Ronquist, F., & Huelsenbeck, J. P. (2003). MRBAYES3: Bayesian phylogenetic inference under mixed models. *Bioinformatics, 19*, 1572–1574.

Santos, M. S. N. (1968). Meloidogyne ardenensis n.sp. (Nematoda: Heteroderidae), a new British species of root-knot nematode. *Nematologica, 13*, 593–598.

Seinhorst, J. W. (1950). De betekenis van de toestand van de grond voor het optreden van aanstasting door het stengelaaltje (*Ditylenchus dipsaci* (Kübn) Filipjev). *Tijdschrift over Plantenziekten, 56*, 292–349.

Seinhorst, J. W. (1962). Modifications of the elutriation method for extracting nematodes from soil. *Nematologica, 8*, 117–128.

Seinhorst, J. W. (1966). Killing nematodes for taxonomic study with hot f.a. 4:1. *Nematologica, 12*, 178.

Siddiqi, M. R. (2000). *Tylenchida parasites of plants and insects* (2nd ed.). Wallingford, UK: CABI.

Swofford, D. L. (2003). *PAUP*. phylogenetic analysis using parsimony (*and other methods), version 4.0b 10*. Sunderland, MA, USA: Sinauer Associates.

Tigano, M. S., Carneiro, R., Jejaprakash, A., Dickson, D. W., & Adams, B. (2005). Phylogeny of *Meloidogyne* spp. based on 18 S rDNA and mitochondrial sequences. *Nematology, 7*, 851–862.

Treub, M. (1885). Onderzoekingen over Sereh-Ziek Suikkeriet gedaan ins Lands Plantentium te Buitenzorg. *Mededeelingen uit's Lands Plantentium, Batavia, 2*, 1–39.

Vrain, T. C., Wakarchuk, D. A., Lévesque, A. C., & Hamilton, R. I. (1992). Intraspecific rDNA restriction fragment length polymorphism in the *Xiphinema americanum* group. *Fundamental and Applied Nematology, 15*, 563–573.

Whitehead, A. G. (1968). Taxonomy of Meloidogyne (Nematodea: Heteroderidae) with descriptions of four new species. *Transactions of the Zoological Society of London, 31*, 263–401.

Yang, B., & Eisenback, J. D. (1983). Meloidogyne enterolobii n. sp. (Meloidogynidae), a root-knot nematode parasitizing pacara earpod tree in China. *Journal of Nematology, 15*, 381–391.

Ziljstra, C., Donkers-Venne, D. T. H. M., & Fargette, M. (2000). Identification of *Meloidogyne incognita*, *M. javanica* and *M. arenaria* using sequence characterised amplified region (SCAR) based PCR assays. *Nematology, 2*, 847–853.